Reprinted from JOURNAL OF APPLIED METEOROLOGY, Vol. 35, No. 4, April 1996
American Meteorological Society

A Comparison of Saturation Pressure Differences and GOES VAS Estimates to Surface Observations of Cloudiness

RANDALL J. ALLISS AND SETHU RAMAN

Department of Marine, Earth and Atmospheric Sciences, North Carolina State University, Raleigh, North Carolina

(Manuscript received 25 April 1995, in final form 11 September 1995)

ABSTRACT

Saturation pressure differences, a measure of parcel saturation, are calculated from upper-air soundings and compared to manual surface observations of cloudiness. The saturation pressure level p^* (more commonly referred to as the lifted condensation level, LCL), can be calculated for each level in a sounding using the temperature and dewpoint temperatures. Thus, p^* of an unsaturated air parcel is found by dry-adiabatic ascent to the pressure level where the parcel is just saturated. The difference between air parcel pressure and saturation pressure level defines the parcel saturation pressure difference. The mean saturation pressure difference between 1000 and 700, 700 and 400, and 400 and 300 mb is calculated and compared to the observed composite cloudiness for those layers. Results indicate that as the absolute value of saturation pressure difference decreases toward zero, the resulting ground observed composite cloud amount increases. However, the mean saturation pressure difference for high clouds ranges from 64 mb under clear skies to 16 mb for overcast conditions. This corresponds to relative humidities between 25% and 76%. Most previous studies do not indicate such large cloud amounts at these humidities. Three empirical relationships that define low, middle, and high clouds are developed based on one year of comparisons. These relationships are then tested on an independent dataset that include a wide variety of cloud cover conditions. Qualitative comparisons are made to manual observations of cloudiness and indicate that the relationships overall slightly overestimate the frequency of cloudiness. Cloudiness derived from the Visible–Infrared Spin Scan Radiometer (VISSR) Atmospheric Sounder (VAS) onboard the Geostationary Environmental Operational Satellite (GOES) 7 using the CO_2 slicing technique is also compared to surface observations. Results indicate that the satellite-derived cloudiness overestimates cloudiness compared with surface observations but is also very similar to the saturation pressure difference estimates.

1. Introduction

Clouds play an important role in the earth's climate system. They affect the earth's radiation budget in both the terrestrial and solar spectra. As a result the formation, maintenance, and dissipation of cloudiness are affected by the radiation and moisture fluxes in the earth's troposphere. Clouds often vary in form, height, and vertical depth. Their phase may also vary from liquid to ice. Furthermore, clouds provide one of the most important mechanisms for the vertical redistribution of momentum, sensible and latent heat on large horizontal scales, influencing the coupling between the atmosphere and the surface as well as the radiative and dynamical balance. Recently, attempts to model cloudiness and cloud processes particularly for use in general circulation models (GCMs) has proven difficult (Randall 1989). This is due to the interaction of clouds with radiative, dynamical and/or hydrological processes on varying timescales. Timescales range from less than one week, in which large-scale dynamical processes dominate (Arakawa and Schubert 1974), to time scales greater than 10 days, in which longwave radiative heat fluxes become increasingly important (Ramanathan 1987).

In many diagnostic cloudiness parameterization schemes, relative humidity is frequently used for estimating the total cloud amount. Many models assume that the fractional area of cloud coverage is determined by the grid-averaged relative humidity. Many formulations assume a threshold relative humidity between 60% and 90% above which partially cloudy conditions can occur. Below these thresholds the algorithms specify clear skies (Walcek 1994). The uncertainty in these cloud cover formulations has stimulated interest in evaluating and improving existing methods for diagnosing cloud cover. Many existing formulations, however, are derived from a limited set of observations used in conjunction with physically intuitive models of cloud formation. In addition, tunable parameters have been introduced in cloud fraction formulations to correspond to a given particular set of observations (Slingo and Slingo 1991).

In this study we attempt to alleviate the problem of limited observations by directly comparing one year of

Corresponding author address: Dr. Sethu Raman, Department of Marine, Earth and Atmospheric Sciences, North Carolina State University, Box 8208, Raleigh, NC 27695-8208.

radiosonde data to surface-observed fractional cloudiness. The data are collected at Cape Hatteras (HAT) and Greensboro (GSO), North Carolina. These two sites fall within a region known as the Gulf Stream Locale (GSL) (Fig. 1). The GSL consists of the mid-Atlantic coastal states from Georgia to Virginia, the adjacent coastal water, the Gulf Stream, and portions of the Sargasso Sea. Figure 1 indicates the location of GSO and HAT as well as a 14-year climatology of sea surface temperatures (SST) within the GSL. The SST is derived from the Miami multichannel sea surface temperature (MCSST) dataset. Recent research has shown that cloudiness in this region exhibits both seasonal and diurnal variations (Alliss and Raman 1995a,b). The seasonal and diurnal variations have also been linked to the interaction of the Gulf Stream, a warm current of water that flows south to north along the U.S. east coast, to the relatively cool adjacent continent. Because of its geography, the atmosphere over the GSL is often baroclinic in nature and produces conditions that are conducive to cloud formation.

Cloudiness on an annual average is observed nearly 75% of the time in this region and is found most often during the winter months. Atmospheric events such as East Coast winter storms and cold air outbreaks are the major producers of clouds during the winter. In a study of the Genesis of Atlantic Lows Experiment (GALE 1986), intensive observation period (IOP) two storm, Alliss and Raman (1995c) documented the relationship between observed cloudiness, as estimated by satellite and ground observations, and related thermodynamics. The saturation point concept, first proposed by Betts (1982), was used to represent the properties of clear and cloudy conditions. The saturation point concept also represents conserved parcel properties by a single point on a thermodynamic diagram. Thus, this parameter may be a useful tool in cloud diagnostic studies. A single linear relationship was derived between the saturation pressure differences and observed composite fractional cloudiness with a correlation of 0.81 estimated.

Although the observations for the GALE case were limited, the high correlation prompted a more in-depth investigation. Accordingly, the aim of this paper is to investigate the relationship between saturation pressure differences and observed fractional cloudiness. Diag-

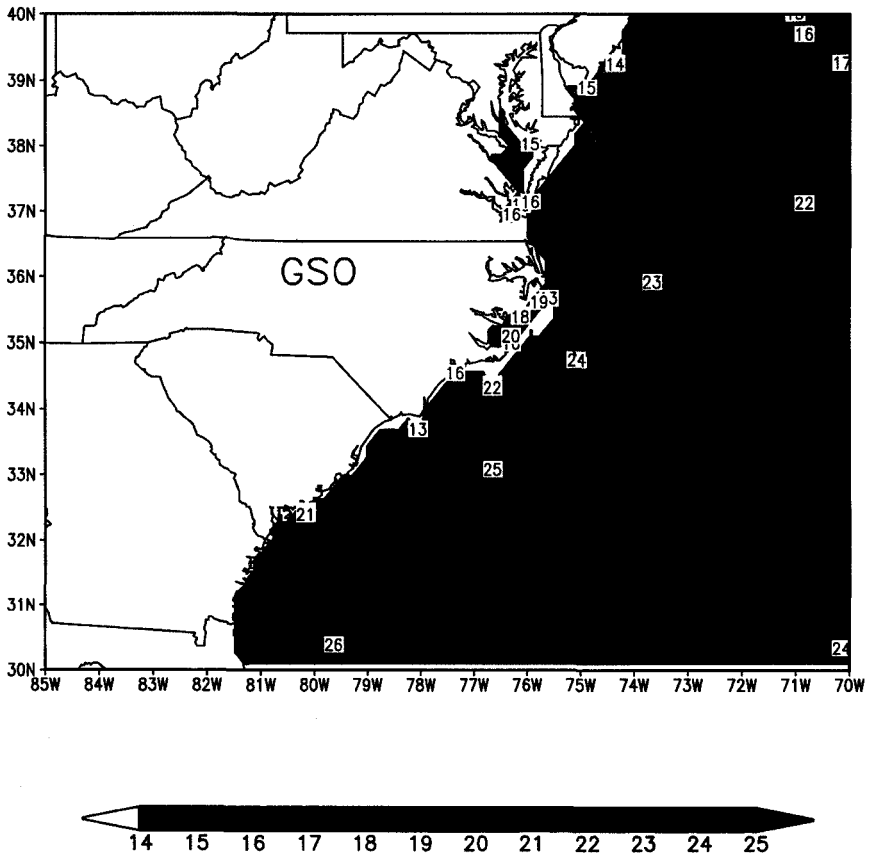

FIG. 1. The geographical location of the Gulf Stream locale. Data used in this study was taken from Greensboro and Cape Hatteras. Also shown is the 1981–94 mean sea surface temperature (°C).

nostic equations are then presented to estimate composite fractional cloudiness given a single atmospheric sounding. A simple test of the equations is provided using an independent dataset that consists of both radiosonde soundings and numerical model analyses. Comparisons are made to satellite cloud heights and amounts using the CO_2 slicing technique.

2. Data and methodology

Upper-air soundings from GSO and HAT are collected between December 1993 and November 1994. The soundings include the standard temperature and moisture products from 1000 to 300 mb and are linearly interpolated to 25-mb levels. The saturation pressure (p^*) level (more commonly referred to as the lifted condensation level, LCL) is calculated for each level in the sounding using the temperature and dewpoint temperatures. Thus, p^* of an unsaturated air parcel is found by dry adiabatic ascent to the pressure level where the parcel is just saturated. On a thermodynamic diagram, air parcels that have a given (T, p) may have saturation levels at any level depending on their total moisture content. The difference between air parcel pressure and saturation pressure level is subsequently estimated and represents the parcel saturation pressure difference (SPD). Parcels with total moisture content greater than $q(T, p)$, where $q(T, p)$ represents the saturation specific humidity at a given temperature and pressure, will be saturated and cloudy with SPD greater than 0. This condition, however, was never found in our soundings. If the parcel total moisture content is less than $q(T, p)$, it will be unsaturated with SPD less than 0. Only if the parcel is just saturated does SPD equal 0. Hence, if a parcel at 700 mb has a p^* of 625 mb, its SPD would be −75 mb. This parcel would therefore need to be lifted 75 mb in order for saturation to take place. Thus, SPD serves as the "potential" for parcel saturation. To facilitate understanding, all references to SPD will be given in terms of its absolute value (thus, −75 mb equals 75 mb). This is done because it is easier to compare SPDs in terms of magnitude rather than more negative or less negative.

The main advantage of using this parameter is that it changes only in proportion to the relative amounts of air undergoing isobaric mixing. In addition, it provides an element of dynamics in the sense that it gives a quantitative indication of how much the parcel must be lifted in order for saturation to occur. Relative humidity on the other hand does not give the same dynamical insight, despite the fact that it is nearly linearly correlated with SPD. In fact, relative humidity, which is directly observed and understood, continues to be used in most cloud diagnostic studies (Walcek 1994). Studies have shown that the total cloud amount can be better estimated as the sum of separate estimates of stratiform and convective cloud amounts using different large-scale parameters than by using a single large-scale variable. The stratiform cloud amount can best be estimated by using relative humidity, while the convective cloud amount can be diagnosed by using a cumulus mass flux (Xu and Krueger 1991). For convenience, however, Fig. 2 shows the relationship between relative humidity and SPD for U.S. standard atmospheric temperature conditions. Because we compare only three-layer mean SPD to the corresponding observed composite cloudiness, only the 1000–700-, 700–400-, and 400–300-mb layer mean SPDs are shown. As one can see, there is a temperature dependence at all levels for these curves. Figure 2 will be referred to throughout the text so that references to relative humidity can be made. It should be stressed that the SPD concept be regarded only as an alternative method in cloud diagnostic studies and not a replacement for the traditionally used relative humidity.

In this study, the mean SPD is calculated for three layers (representing different cloud height categories) in a given sounding: 1000–700 mb (low clouds), 700–400 mb (midlevel clouds), 400–300 mb (high clouds), and 1000–300 mb (clear sky). This is done to directly compare with surface observations of cloudiness. The surface airway observations (SAO) from GSO and HAT are also collected for the December 1993–November 1994 period. They include manual observations of clouds in multiple layers estimated from the perspective of a ground observer. Cloud base height (in feet) and amount of cloud coverage are reported. Cloud fraction from the SAO are reported in four categories: clear (CLR), for a sky coverage of less than one-tenth; scattered (SCT), defined as one- to five-tenths coverage; broken (BKN), defined as five- to nine-tenths sky cover; and overcast (OVC), reported when clouds cover more than nine-tenths of the sky. Cloud heights observed by the ground observer

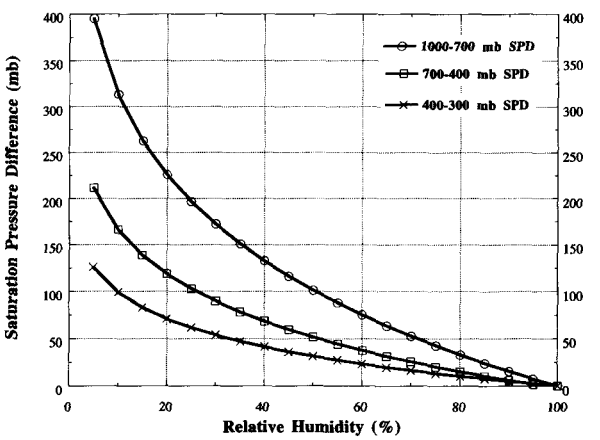

FIG. 2. The relationship between the saturation pressure difference and relative humidity for U.S. standard atmospheric conditions. The curves represent the 1000–700-, 700–400-, and 400–300-mb layers, respectively. There is a temperature dependence at all levels for these curves.

are reported from low to high. In this study, low clouds are defined as cloud bases less than 10 000 feet (~1000–700 mb), midlevel clouds are defined as cloud bases between 10 000 and 20 000 feet (~700–400 mb), and high clouds, defined as cloud bases greater than 20 000 feet (~400–300 mb). The pressure levels represent the approximate ranges of the cloud height categories reported by the ground observer. Unfortunately, both cloud heights and fractions are limited to three and four categories, respectively. Clearly, fractional cloudiness reported in tenths would be more useful. The lack of resolution therefore represents one limitation but not a fatal flaw.

In order to simply the comparisons, a "composite" cloud fraction is calculated for each SAO cloud height category. For example, if the ground observer reports SCT and BKN low clouds and OVC high clouds, two composite cloud reports are made. The composite cloud reports are constructed by choosing the greatest cloud fraction within each height category. Thus, in this case, a low BKN and high OVC would serve as the composite cloud fractions. If the ground observer reports midlevel OVC, then OVC conditions represent the composite cloud fraction for the midlevels. The mean SPD for each cloud height category are also calculated for clear sky observations. Table 1 lists the nine composite cloud fraction categories used in the analysis. Also listed is the percentage each category is represented in the 1-yr dataset. As Table 1 indicates, cloudiness is observed nearly three-quarters of the time during this period. Only 27% of the observations are identified as clear sky. Comparisons are limited to 0000 and 1200 UTC, the standard synoptic times. Along the East Coast this corresponds to 1900 and 0700 EST. During the late fall through early spring, the 0000 UTC observation will occur just after dusk at both GSO and HAT. According to Hahn et al. (1995), a bias in underestimating middle and high cloudiness by surface observers may be present at these times. To correct for this if the ground observer reported anything less than overcast conditions for a layer, then the observation was thrown out. Nearly 1500 soundings were collected, of which 1260 were of sufficient quality to be used in the analysis. Another important assumption is that the upper-air soundings are assumed to represent the field of view of the surface observers. In this case, the mean horizontal visibility reported by the observers was approximately 20 km and was therefore used to represent the resolution of the cloud coverage assigned to the mean SPD.

Satellite-derived cloudiness is also used to compare with surface cloud estimates. The Visible–Infrared Spin Scan Radiometer (VISSR) Atmospheric Sounder (VAS) CO_2 slicing technique is used to calculate cloud-top pressures (CTP) and effective cloud amounts. This dataset is a subset of the satellite-derived North American cloud climatology produced at the University of Wisconsin and documented in Wylie and Menzel (1989) and Menzel et al. (1992). Cloud-top pressures are available at 50-mb intervals between 1000 and 100 mb. The CO_2 slicing technique is used to derive heights above 700 mb. This technique takes advantage of the partial CO_2 absorption in three of the IR channels, with each channel sensitive to a different level in the atmosphere. Low clouds (CTP > 700 mb) are determined through a comparison of the 11.2-μm window channel radiances and an in situ temperature profile. Once a cloud height is determined, an effective cloud amount is evaluated from the IR window channel. The effective cloud amount is defined as the ratio of the radiance difference the observed cloud produces to the radiance difference an opaque cloud at the same level would produce in the infrared window. VAS data are available at approximately 0000 and 1200 UTC. A more complete documentation of this technique including errors and limitations may be found in the cited references.

TABLE 1. The percent each cloud category, including clear sky, is observed between December 1993 and November 1994.

	Clear Sky (CLR)	Scattered (SCT)	Broken (BKN)	Overcast (OVC)
Clear sky	27	NA	NA	NA
Low	NA	3	8	22
Middle	NA	2	3	10
High	NA	9	4	12

NA, not applicable.

3. Averaging of data in cloudiness regimes

As alluded to in section 2, frequency distributions of the mean SPDs are investigated for patterns that can reveal the ground-observed fractional cloudiness by evaluating each cloud height category and composite fraction separately. The mean SPD readily distinguishes clear from cloudy conditions. In addition, they exhibit strong features that can be used to recognize composite overcast clouds at all three levels. For scattered and broken cloud conditions the signals are not as strong. Figures 3–6 summarize the results of the comparisons. The values represent the frequency that the composite cloud fraction/height fell within the specified SPD intervals. Figure 3 shows the frequency distribution of the mean SPD between 1000 and 300 mb for ground reports of clear sky. Clear sky conditions are found most often when the SPD is greater than 50 mb. This corresponds to a relative humidity below 50%. During overcast conditions, the SPD is predominantly found in the 0–10-mb range for low clouds and 10–20 mb for mid- and high-level clouds. As one can see from Fig. 4, the SPD values correspond to different relative humidity ranges depending on the level. For instance, at a SPD of 10 mb the range in relative hu-

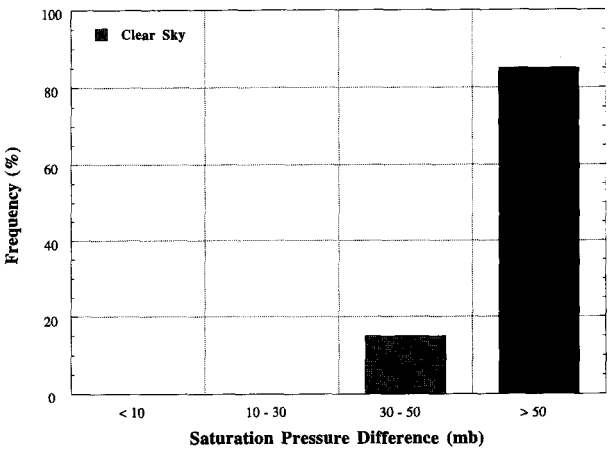

FIG. 3. The frequency distribution of the mean SPD for ground observations of clear sky for the 12-month period between December 1993 and November 1994.

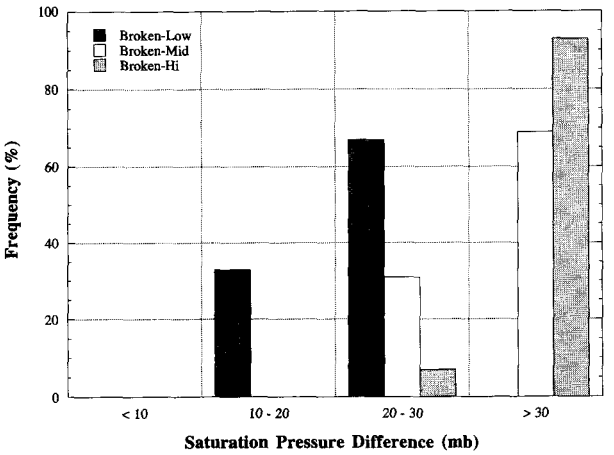

FIG. 5. Same as Fig. 4 except for (a) low-level broken clouds, (b) midlevel broken clouds, and (c) high-level broken clouds.

midity between the mid- and high-level categories is 5%, whereas at 20 mb the range is approximately 10%.

Comparisons when the ground observer reports broken cloudiness are shown in Fig. 5. The overall magnitude of SPD during broken sky conditions is greater for midlevel clouds than for low clouds. This is indicative of lower relative humidities. The increase in SPD in this case may be a function of a reduced cloud fraction. However, Fig. 5 does indicate that the SPD also increases with increasing cloud height. Theoretically, this would mean that for a given cloud fraction, the relative humidity would decrease with height. However, because this should not be possible, the other possibility is the inability of the sensor to accurately detect moisture at upper levels.

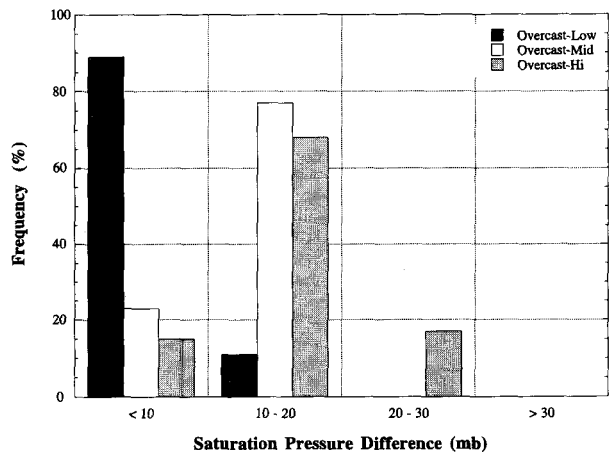

FIG. 4. Frequency distribution of the mean SPD for ground observations (%) of overcast sky less than 10 000 ft for the 12-month period between December 1993 and November 1994. (b) Overcast midlevel clouds between 10 000 and 20 000 ft. (c) Overcast high-level clouds greater than 20 000 ft.

The same trend is also evident in Fig. 6, which shows the frequency distributions when scattered clouds are observed. In this case, scattered clouds are never observed at SPD less than 30 mb, which for low clouds corresponds to a humidity of 82%. Although scattered clouds at midlevels are reported most often at SPD greater than those for high-level clouds, the corresponding relative humidities are still higher. Comparisons are also made when precipitation was reported in the SAO (not shown). When the SAO indicates precipitation, the mean SPD in the 1000–700-mb layer is greater than 10 mb nearly 99% of the time. This indicates a deep layer of nearly saturated conditions and thus may serve as a possible indicator of precipitation.

Table 2 gives the mean and standard deviations of the SPD for each composite cloud fraction category as a function of height. For comparison purposes, the corresponding mean relative humidity is computed and

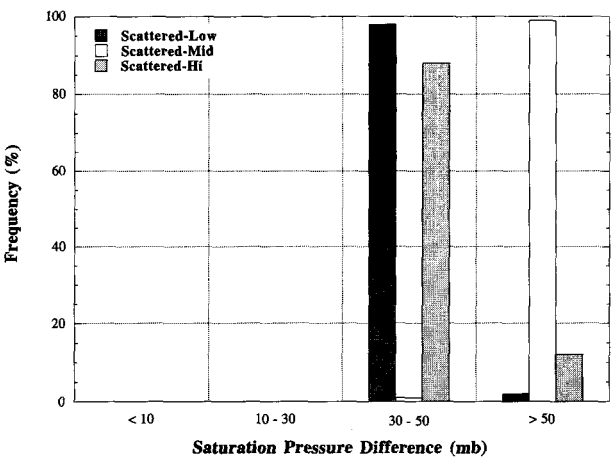

FIG. 6. Same as Fig. 4 except for (a) low-level scattered clouds, (b) midlevel scattered clouds, and (c) high-level scattered clouds.

TABLE 2. The mean and standard deviations of SPD when low, middle, and high scattered, broken, and overcast conditions are found.

Cloud fraction	Mean SPD (mb)	Standard deviation (mb)	Mean relative humidity (%)
Low clouds 1000–700 mb			
CLR	104.0	13.6	49
SCT	41.4	8.6	78
BKN	21.4	4.2	87
OVC	7.1	2.6	100
Middle clouds 700–400 mb			
CLR	88.6	15.5	34
SCT	61.8	10.1	49
BKN	26.2	5.6	74
OVC	12.1	3.3	87
High clouds 400–300 mb			
CLR	64.2	5.4	25
SCT	48.7	5.2	36
BKN	34.8	5.3	48
OVC	15.8	3.5	76

Clear-sky means and standard deviations are also included. For comparison purposes the corresponding mean relative humidity is presented.

shown. The mean SPD when the surface observer reports clear skies is also given for each height category. For low cloudiness, the mean SPD ranges from 104 mb under clear conditions to 7 mb for overcast conditions. The standard deviation generally increases with decreasing composite cloud cover. This is not surprising because large variations in moisture content for a layer may be present during clear sky conditions. There is also a significant gap between clear sky and scattered cloudiness with the mean SPD decreasing by more than a factor of 2. The corresponding relative humidity for the 1000–700-mb layer ranges from 50% to nearly 100%. This range in relative humidity agrees with several cloud fraction formulations presented in Fig. 1 of Walcek (1994). In that study, six formulations used by meso- and global-scale numerical models indicate fractional cloud coverage at 800 mb increases from 60% for clear skies to 100% for overcast conditions.

For midlevel clouds, SPD ranges from near 90 mb under clear conditions to 12 mb when composite overcast conditions are reported. This corresponds to mean humidities between 35% and 87%. Thus, compared with low-cloud reports, SPDs and its associated relative humidity are observed at higher (lower) values. The standard deviations are larger for midlevel clouds than for low-level clouds; however, little overlap between the composite cloud fraction categories is present, indicating that these clouds are observed at discreet values of SPD. The mean SPD for high cloudiness ranges from 64 mb under clear skies to 16 mb for overcast

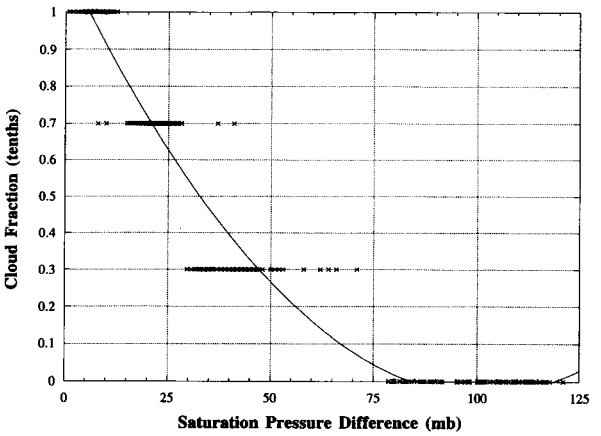

FIG. 7. Scatterplot of the mean SPD as a function of the observed low-level composite fractional cloudiness. A second-order polynomial is used to fit the data.

conditions. This is an interesting result because these values correspond to mean relative humidities between 25% and 76% for clear and overcast conditions, respectively. Most previous studies do not indicate such large cloud fractions at these humidity values. We suspect that the moisture sensor may be failing at these altitudes resulting in much higher (lower) than expected SPD (relative humidities).

4. Cloud fraction relationships

Based on the comparisons presented in section 3, statistical relationships are derived between the SPD and the composite cloud fractions. Figure 7 shows a scatterplot of the mean SPD for low-level cloudiness as a function of observed composite cloud fraction. A second-order polynomial is used to fit the data, which yields a correlation of 0.88. Even though only four cloud fractions are used in the comparison the fit allows

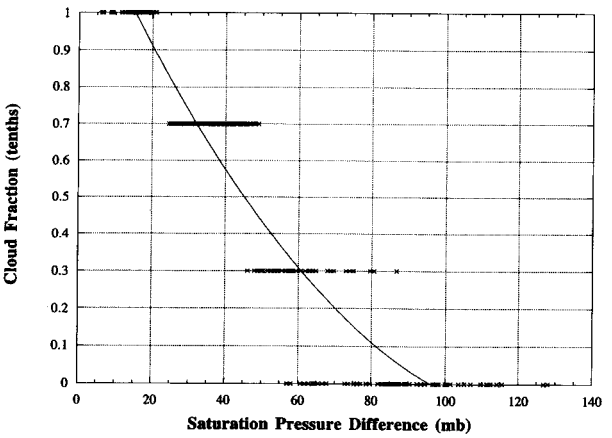

FIG. 8. Same as Fig. 7 except for midlevel clouds. A second-order polynomial is used to fit the data.

for a continuous relationship. As alluded to earlier, a distinct decrease in the SPD between clear and scattered conditions is present in the comparisons. Figure 8 shows the scatterplot for midlevel cloudiness. Clear sky observations (at midlevels) show a larger spread than the low-level category, and the data appear to overlap with scattered conditions. As is the case with low-level fractional cloudiness, broken and overcast conditions at midlevels fall in discreet ranges with little overlap between the two categories noted. A second-order polynomial is also used to fit the data and yields a correlation of 0.91. The comparison between SPD and the composite cloud fraction for high-level clouds is given in Fig. 9. For high clouds, there is a tendency for more overlap of the data between cloud fraction categories despite the small standard deviations. Nevertheless a correlation of 0.90 is calculated. For consistency, a second-order polynomial is also used to fit the data; however, a linear fit gives a similar result. It is noteworthy to mention that the range of SPD (relative humidity) for high clouds is less (more) than for mid- or low-level clouds. This may be associated with the sensor's reduced capability of accurately measuring moisture at higher levels. It is widely accepted that high clouds (cirrus) are not observed reliably at night and are often dropped or added to the observed cloud field at "first light." This may affect our 1200 UTC observations during winter and may also have an influence on the more linear curve for high clouds shown in Fig. 9. These human limitations, compounded by the rawinsonde instrument limitations at high altitudes, may both have an impact on these correlations.

The following equations represent the second-order polynomials that are used to fit the data. Because of the lack of resolution in manual observations of fractional cloud cover, these equations are presented only as preliminary guidelines for calculating a composite cloud fraction for a layer.

For low-level clouds, where SPD_{low} is the mean SPD between 1000 and 700 mb,

$$f(SPD_{low}) = 1.129 + 0.022(SPD_{low}) + 11.294 \times 10^{-5}(SPD_{low})^2 \quad (1)$$

$$\text{if} \quad SPD_{low} < 5 \text{ mb}, \quad f(SPD_{low}) = 1.0$$

$$\text{if} \quad SPD_{low} > 80 \text{ mb}, \quad f(SPD_{low}) = 0.0.$$

For midlevel clouds, where SPD_{mid} is the mean SPD between 700 and 400 mb,

$$f(SPD_{mid}) = 1.315 - 0.022(SPD_{mid}) + 8.574 \times 10^{-5}(SPD_{mid})^2 \quad (2)$$

$$\text{if} \quad SPD_{mid} < 15 \text{ mb}, \quad f(SPD_{mid}) = 1.0$$

$$\text{if} \quad SPD_{mid} > 95 \text{ mb}, \quad f(SPD_{mid}) = 0.0.$$

For high-level clouds, where SPD_{hi} is the mean SPD between 400 and 300 mb,

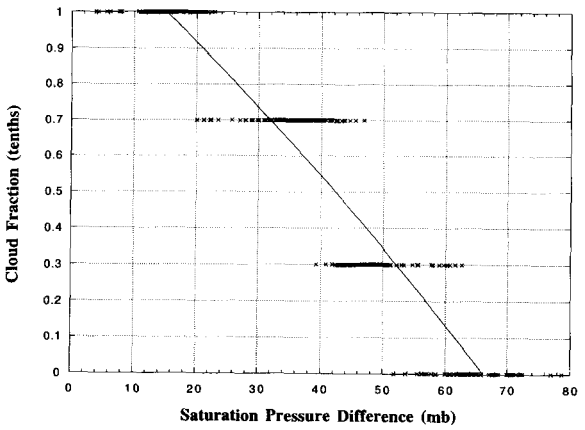

FIG. 9. Same as Fig. 7 except for high-level clouds. A second-order polynomial is used to fit the data.

$$f(SPD_{hi}) = 1.245 - 0.015(SPD_{hi}) - 5.183 \times 10^{-5}(SPD_{hi})^2 \quad (3)$$

$$\text{if} \quad SPD_{hi} < 20 \text{ mb}, \quad f(SPD_{hi}) = 1.0$$

$$\text{if} \quad SPD_{hi} > 65 \text{ mb}, \quad f(SPD_{hi}) = 0.0.$$

The symbol f is used to represent the composite cloud fraction. Occasionally, values of SPD will result in a composite cloud fraction greater than 1.0 or less than 0.0. In these situations, the resulting composite cloud fraction is assumed to be overcast if f is greater than 1.0 and clear if f less than 0. If the three SPDs calculated from a sounding are all less than one-tenth, then the total cloud amount is assumed to be zero.

An independent test of the equations is performed using SPD derived from upper-air soundings at GSO and HAT for the month of December 1994. In addition, SPD are derived from the National Meteorological Center's (NMC) eta step-mountain coordinate model analyses to also estimate composite fractional cloudiness at these sites. The eta model has acquired the name of its vertical coordinate, the Greek letter eta. The eta coordinate system is actually only a simple variation of the commonly used sigma coordinate system formerly employed by NMC in the Limited-Area Fine-Mesh (LFM) model, the Nested Grid Model (NGM), and the global spectral model. Both coordinate systems are normalized and pressure based. However, while the sigma coordinate varies from 0 to 1 between the top of the model domain and the model's ground surface, the eta coordinate varies from 0 to 1 between the top of the model's vertical domain (currently 50 mb) and mean sea level. The result is that all of the eta coordinate surfaces tend to be nearly horizontal in all circumstances, which can produce a significant numerical benefit when computing the pressure-gradient force near steep terrain where the sigma coordinate must be sloped. Given this horizontal nature of eta, it seems

natural to render the model's topography into the shape of steps, hence the term step-mountain. The eta model analyses provide temperature and dewpoint temperatures at 50-mb vertical resolution that are used to calculate p^* and SPD. For a complete description of the eta model the reader is referred to Mesinger et al. (1988).

The manual surface reports from GSO and HAT are used to compare with the derived composite fractional cloudiness. Because the manual observations have a coarse resolution in cloud cover, we do not attempt to use them directly for verification; rather, a qualitative comparison is presented. This month presents a variety of cloud types and cloud amounts, so that different weather conditions are well represented. As in the case for the 1-yr study only the 0000 and 1200 UTC upper-air soundings and eta model analyses are used. Figure 10a shows the frequency distribution of the composite low-level fractional cloudiness using the relationship in Eq. (1). The frequency of clear-sky observations when the three equations indicate a cloud fraction less than one-tenth are also shown in Fig. 10a. The remaining distributions have been aggregated into five two-tenth interval cloud fraction classifications. Estimates made from upper-air and eta model–derived SPD indicate cloud amounts less than one-tenth and greater than nine-tenths are found most often. These two categories makeup nearly 45% of all observations. There is a slight tendency for the upper-air soundings to overestimate cloudiness relative to estimates from eta model analyses. Low-level clouds between one- and nine-tenths make up only 8% of the observations during December 1994. For comparison purposes, Fig. 10b shows the surface observed estimates of low-level cloud amount from GSO and HAT during December. As indicated earlier, manual observations of cloud amount are limited to four categories including clear skies, scattered, broken, and overcast conditions. Therefore, direct comparisons are impossible. However, as Fig. 10b indicates, there is a tendency for clear skies and overcast low clouds to dominate. Overall, it appears that the SPD estimates of clear sky are under represented compared with manual observations, indicating a slight bias toward overestimating cloud amounts. Compared to manual observations, the SPD technique under estimates low-level clouds by nearly 7%. Due to the limited comparisons, it is uncertain whether this is a true bias. It is not surprising, however, that both manual observations and SPD-derived overcast low clouds are represented more often than any other height/amount category because rainfall during this month was above normal at both stations.

Figure 11a shows the estimates of cloud amount for midlevel clouds based on the relationship found in Eq. (2). Midlevel cloud amounts from one- to nine-tenths are found only 16% of the time. Furthermore, all five categories are represented about equally except for the highest cloud amount category, which is represented

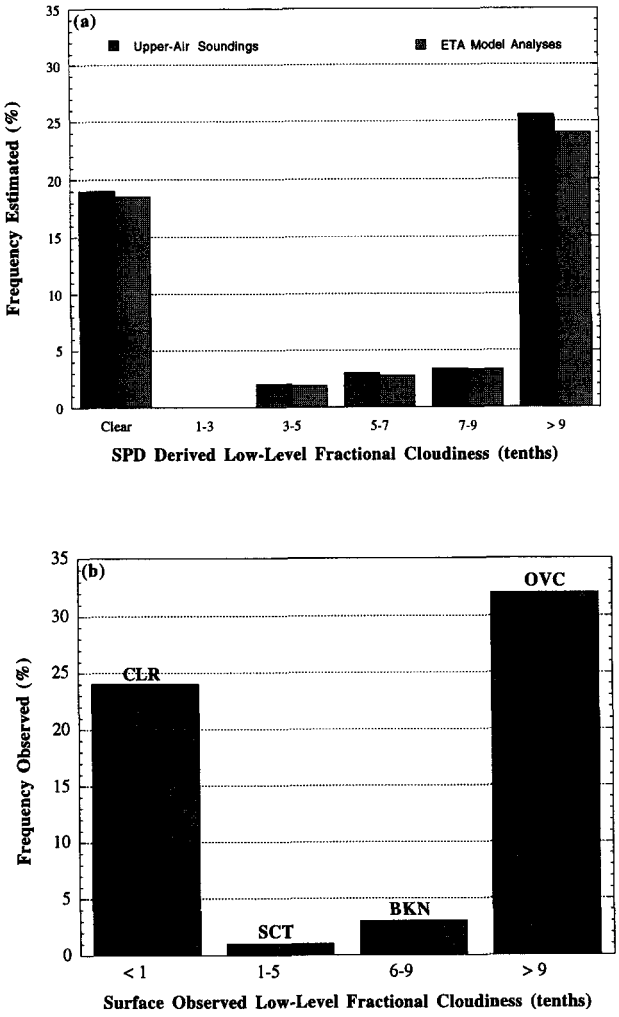

FIG. 10. (a) The December 1994 estimated frequency of low-level cloudiness as a function of cloud fraction derived from Eq. (1) using upper-air and eta model analyses of saturation pressure differences. (b) The frequency of low-level cloudiness as a function of cloud fraction estimated by surface observers. Estimates for clear sky conditions are also included.

slightly more during this month. Upper-air soundings and eta model analyses indicate the same distributions. Manual observations indicate that midlevel clouds are found 14% of the time with 8% of the observations reported as overcast (Fig. 11b). The overall tendency for manual observations to be reported slightly less than the SPD estimates may be a function of the inability of the surface observer to see midlevel clouds due to the high amounts of low clouds. As is the case with low clouds, the SPD estimates of midlevel cloud amount greater than nine-tenths is underreported compared with manual observations, albeit by only 2%–3%.

The distribution of cloud amount for high-level clouds as derived using Eq. (3) is shown in Fig. 12a.

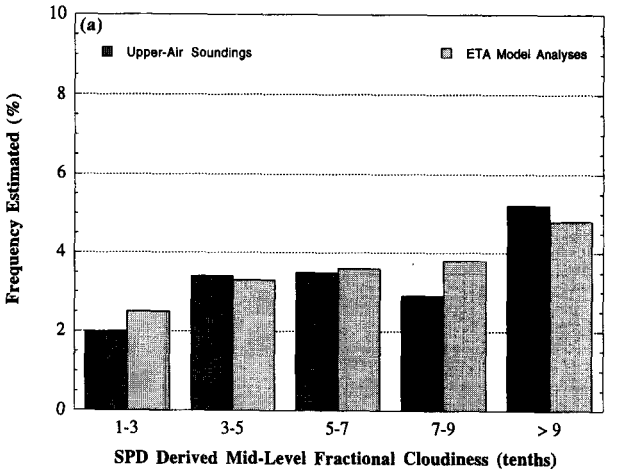

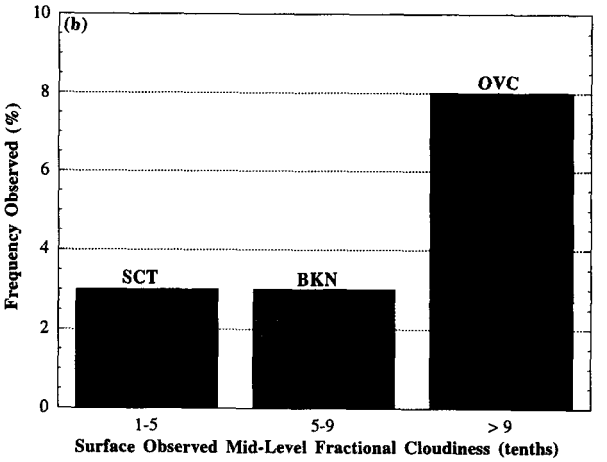

FIG. 11. (a) Same as Fig. 10a except for midlevel clouds using Eq. (2). (b) Same as Fig. 10b except for surface observed midlevel clouds.

An increasing frequency of cloud amount is noted with upper-air soundings and eta model analyses showing similar frequencies. Overall high-level clouds are estimated 30% of the time during December 1994 with nearly half showing a cloud amount greater than nine-tenths. Manual observations indicate high clouds are present 26% of the time, slightly lower than the SPD estimates (Fig. 12b). Compared to manual observations, the SPD-derived cloud amounts greater than nine-tenths are under-reported. There is also a tendency for Eq. (3) to report more clouds in the three- to nine-tenths category. Despite these discrepancies the overall distribution is consistent with manual observations.

As mentioned in section 2, VAS cloud heights (cloud-top pressure, CTP) and effective cloud amounts are used to compare with surface reports and upper-air (eta) estimates of composite cloud amount during the month of December 1994. The term "frequency of cloudiness" is used to describe the satellite-derived cloudiness. By statistically segmenting the satellite cloud heights and effective cloud amounts, useful comparisons can be made to surface observations. A statistical summary of all cloud observations obtained in a 50 km × 50 km grid over GSO and HAT at 0000 and 1200 UTC are shown in Table 3. Approximately 3100 observations were processed during this period. Because of the relatively large sample size and the accuracy of the CO_2 slicing technique, entries in Table 3 are accurate to within 1% (Menzel et al. 1992). Evaluations are subdivided into four categories based on cloud height. High clouds are defined as CTP < 400 mb. Midlevel clouds are defined as CTP between 400 and 700 mb. CTP greater than 700 mb include the correct identification of low opaque clouds, evaluation of ground as low cloud, and the incorrect identification of broken or scattered low clouds as opaque cloud. Cloud-free conditions are labeled as clear sky. An "X" is used

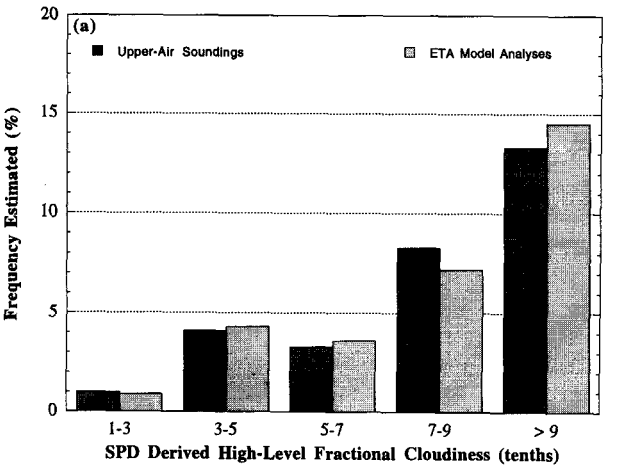

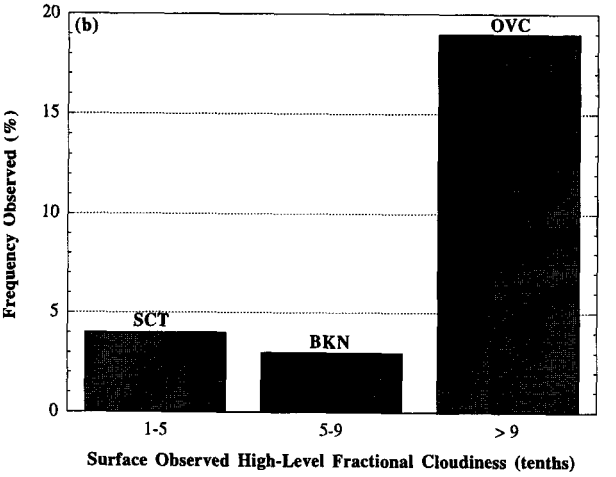

FIG. 12. (a) Same as Fig. 10a except for high-level clouds using Eq. (3). (b) Same as Fig. 10b except for surface observed high-level clouds.

to indicate where VAS does not provide any information. The effective cloud amount is subdivided into four categories shown in each column of Table 3. The right column contains the opaque or nearly opaque cloud reports. As defined in Wylie and Menzel (1989), effective cloud amounts greater than 0.95 are considered to be opaque because cloud-top heights derived from the CO_2 slicing algorithm are very close to heights derived from the IR window channel. The remaining three columns separate the effective cloud amounts ranging from thin high- and midlevel clouds in column 1 to thick high- and midlevel clouds in column 3. The effective cloud amount for an opaque overcast cloud should be nearly 1.0 and should be 0 for clear skies. Table 3 indicates that sky conditions were quite cloudy during December 1994 with only 20.5% of the observations identified as clear sky. High clouds (sum of row 1) are estimated approximately 27.6% of the time and midlevel clouds (sum of row 2) 17.7%. Low opaque clouds are identified 34.2% of the time. Of the 45.3% of the total high and midlevel clouds observed, 28.1% are determined to be semitransparent to terrestrial radiation (effective cloud amount less than 0.95). This estimate is similar to the 26% found over most of North America by Menzel et al. (1992) using four years of VAS observations.

For comparison purposes, Fig. 13 shows the frequency of occurrence of the three cloud heights used in this study and also clear sky conditions. Cloud frequencies derived from VAS, upper-air (eta), and manual observations are shown. The data are aggregated according to cloud height to facilitate the comparison. VAS reports are remarkably similar to manual observations of cloudiness during December 1994. As Fig. 12 shows, VAS estimates of clear sky are indicated 20% of the time compared to the 24% reported by the surface observer. The difference may be associated with the underestimate of clear sky by the satellite technique due to the erroneous evaluation of ground as low clouds. This is a problem mainly in the morning hours during winter and represents up to a 5% under estimate in clear sky (Alliss and Raman 1995a). SPD-derived clear-sky estimates are also similar to VAS observations. While estimates of the frequency of low clouds by all three sources are less than surface observations, an overestimate exists for both mid- and high-level clouds. We believe that at least part of this difference is an artifact because the ground observer will under report mid- and high-level clouds when overcast low clouds are present. Nevertheless, estimates for all three cloud height categories are within 2%–4% of surface estimates. In this particular illustration, the SPD and VAS cloud amounts agree qualitatively with surface estimates, but further test and refinements of the relationships are required.

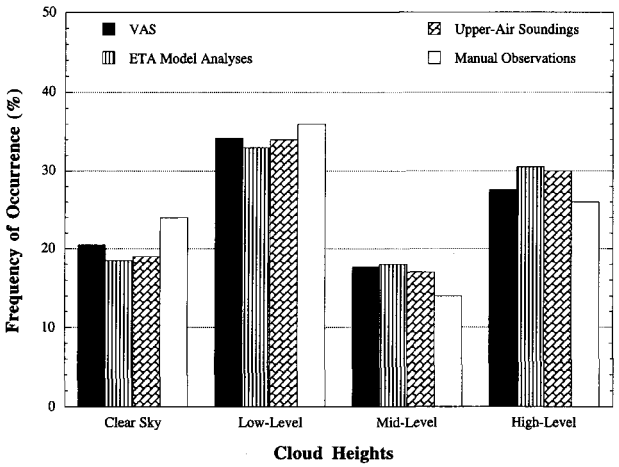

FIG. 13. A comparison of the frequency of occurrence of cloudiness at GSO and HAT as derived from VAS, upper-air soundings and eta model analyses during the month of December 1994. The manual observations taken from these locations are also shown.

5. Conclusions

Profiles of SPD, obtained from upper-air soundings, were used to compare with surface observations of cloud cover. Patterns of saturation pressure differences that could reveal the ground observations were investigated. The method makes several simplifying assumptions. Ground observations of cloud cover are grouped into three height categories (low, middle, and high) with the greatest cloud fraction in each height category representing the "composite" cloud amount for that height group. If only one cloud fraction is indicated in the surface report (for a given height category), then it is used to represent the entire layer. Ob-

TABLE 3. The mean frequency of occurrence of cloudiness as a function of effective cloud amount for December 1994 at GSO and HAT.

Cloud-top pressure (CTP)	Effective cloud amount (%)			
	0.00–0.33	0.34–0.65	0.66–0.95	0.96–1.00
CTP < 400 mb	3.9	5.9	8.8	9.0
400 mb ≤ CTP < 700 mb	1.1	3.5	4.9	8.2
CTP ≥ 700 mb	X	X	X	34.2
Clear sky	20.5	X	X	X

An "X" denotes where no additional cloud information is possible. Entries in Table 3 are accurate to within 1%.

servations show that as the saturation pressure difference increases, the observed cloud amount increases. The comparisons also indicate that the mean saturation pressure difference for high clouds ranges from 64 mb under clear skies to 16 mb for overcast conditions. This corresponds to relative humidities between 25% and 76%. Most previous studies do not indicate such large cloud amounts at these humidities. A second-order polynomial relationship was developed for each cloud height category on the basis of these observations. These equations were then tested on an independent dataset and then qualitatively compared to surface observations. Because there was a lack of resolution in the manual observations of cloud amount, direct one-to-one comparisons could not be made. Results indicate that SPD cloud amounts at all height levels agreed qualitatively with surface observations. Overall clear-sky observations were reported 24% of the time by the surface observer compared to 19% derived from SPD. There was a tendency for the low-level clouds to be underreported by the SPD method but an overestimate existed at middle and high levels. This overestimate may be an artifact because the ground observer under reports mid- and high-level clouds when overcast low clouds are present. Cloud amounts were also calculated from GOES VAS using the CO_2 slicing technique. VAS-derived cloud amounts were similar to surface reports with only a slight overestimate in cloudiness evident in the statistics. This overestimate was due primarily to the inability of VAS to distinguish clear sky from low clouds during the morning hours of the winter months.

This study has presented an alternative method in studying fractional cloudiness through the use of the saturation pressure difference concept. Because this parameter is derived directly from relative humidity, it is not suggested as a replacement but merely a way to quantitatively gauge the subsaturation of a parcel and to indicate how much lifting is needed for saturation to occur. Furthermore, the saturation pressure difference along with relative humidity provides more evidence of the lack of reliable moisture measurements at levels where high clouds are observed.

Acknowledgments. The authors express their gratitude to Don Wylie of the Space Science and Engineering Center, University of Wisconsin–Madison for providing us with the VAS cloud height dataset. This work was supported by the Department of Energy's Atmospheric Radiation Measurement program under Contract 091575-A-Q1 with Pacific Northwest Laboratories.

REFERENCES

Alliss, R. J., and S. Raman, 1995a: Quantitative estimates of cloudiness over the Gulf Stream locale using GOES VAS observations. *J. Appl. Meteor.*, **34,** 500–510.

——, and ——, 1995b: Diurnal variations in cloudiness over the Gulf Stream locale. *J. Appl. Meteor.*, **34,** 1578–1594.

——, and ——, 1995c: Cloudiness and its relationship to saturation pressure differences during a developing East Coast winter storm. *J. Appl. Meteor.*, **34,** 2367–2387.

Arakawa, A., and W. H. Schubert, 1974: Interaction of a cumulus cloud ensemble with the large-scale environment. Part I: *J. Atmos. Sci.*, **31,** 674–701.

Betts, A. K., 1982: Saturation point analysis of moist convective overturning. *J. Atmos. Sci.*, **39,** 1484–1505.

Hahn, C. J., S. G. Warren, and J. London, 1995: The effect of moonlight on observation of cloud cover at night, and application to cloud climatology. *J. Climate,* **8,** 1429–1446.

Menzel, W. P., D. P. Wylie, and K. I. Strabala, 1992: Seasonal and diurnal changes in cirrus clouds as seen in four years of observations with VAS. *J. Appl. Meteor.*, **31,** 370–385.

Mesinger, F., Z. I. Janjic, S. Nickovic, D. Gavrilov, and D. G. Deaven, 1988: The step-mountain coordinate: Model description and performance for cases of alpine lee cyclogenesis and for a case of an Appalachian redevelopment. *Mon. Wea. Rev.*, **116,** 1493–1518.

Ramanathan, V., 1987: The role of earth radiation budget studies in climate and general circulation research. *J. Geophys. Res.*, **92,** 4075–4095.

Randall, D. A., 1989: Cloud parameterization for climate modeling; stratus and prospects. *Atmos. Res.*, **23,** 345–361.

Slingo, A., and J. M. Slingo, 1991: Response of the National Center for Atmospheric Research Community Climate Model to improvements in the representation of clouds. *J. Geophys. Res.*, **96,** 15 341–15 357.

Walcek, C. J., 1994: Cloud cover and its relationship to relative humidity during a springtime midlatitude cyclone. *Mon. Wea. Rev.*, **122,** 1021–1035.

Wylie, D. P., and W. P. Menzel, 1989: Two years of cloud cover statistics using VAS. *J. Climate Appl. Meteor.*, **2,** 380–392.

Xu, K.-M., and S. K. Krueger, 1991: Evaluation of cloudiness parameterizations using a cumulus ensemble model. *Mon. Wea. Rev.*, **119,** 342–367.